

# Fractional Laser-Assisted Drug Delivery: Active Filling of Laser Channels With Pressure and Vacuum Alteration

Andrés M. Erlendsson, MD,<sup>1,2\*</sup> Apostolos G. Doukas, PhD,<sup>1</sup> William A. Farinelli, BA,<sup>1</sup> Brijesh Bhayana, PhD,<sup>1</sup> R. Rox Anderson, MD,<sup>1</sup> and Merete Haedersdal, DMSc<sup>1,2</sup>

<sup>1</sup>Wellman Center for Photomedicine, Massachusetts General Hospital, Harvard Medical School, Boston, Massachusetts 02114

<sup>2</sup>Department of Dermatology, Bispebjerg University Hospital, Copenhagen, Denmark

**Background and Objective:** Ablative fractional laser (AFXL) is rapidly evolving as one of the foremost techniques for cutaneous drug delivery. While AFXL has effectively improved topical drug-induced clearance rates of actinic keratosis, treatment of basal cell carcinomas (BCCs) has been challenging, potentially due to insufficient drug uptake in deeper skin layers. This study sought to investigate a standardized method to actively fill laser-generated channels by altering pressure, vacuum, and pressure (PVP), enquiring its effect on (i) relative filling of individual laser channels; (ii) cutaneous deposition and delivery kinetics; (iii) biodistribution and diffusion pattern, estimated by mathematical simulation.

**Methods:** Franz diffusion chambers (FCs) were used to evaluate the PVP-technique, comparing passive (AFXL) and active (AFXL + PVP) channel filling. A fractional CO<sub>2</sub>-laser generated superficial (225 μm; 17.5 mJ/channel) and deep (1200 μm; 130.5 mJ/channel) channels, and PVP was delivered as a 3-minutes cycle of 1 minute pressure (+1.0 atm), 1 minute vacuum (−1.0 atm), and 1 minute pressure (+1.0 atm). Filling of laser channels was visualized with a colored biomarker liquid ( $n = 12$  FCs,  $n = 588$  channels). Nuclear magnetic resonance quantified intracutaneous deposition of topically applied polyethylene glycol (PEG400) over time (10 minutes, 1 hour, and 4 hours), investigated with ( $n = 36$  FCs) and without ( $n = 30$  FCs) PVP-filling. Two-dimensional mathematical simulation was used to simulate intradermal biodistribution and diffusion at a depth of 1,000 μm.

**Results:** Active filling with application of PVP increased the number of filled laser channels. At a depth of 1,000 μm, filling increased from 44% (AFXL) to 94% with one PVP cycle (AFXL + PVP;  $P < 0.01$ ). Active filling greatly enhanced intracutaneous deposition of PEG400, resulting in a rapid delivery six-folding uptake at 10 minutes (AFXL 54 μg/ml vs. AFXL + PVP 303 μg/ml,  $P < 0.01$ ). AFXL alone generated an inhomogeneous uptake of PEG400, which greatly improved with active filling, resulting in a uniform uptake within the entire tissue.

**Conclusion:** Active filling with PVP secures filling of laser channels and induces a deeper, greater, more rapid delivery than conventional AFXL. This delivery technique has promise to improve treatment efficacy for

medical treatments of dermally invasive lesions, such as BCCs. *Lasers Surg. Med.* 48:116–124, 2016.

© 2015 Wiley Periodicals, Inc.

**Key words:** active filling; drug delivery; laser; laser-assisted drug delivery

## INTRODUCTION

Topical drug application is the most common treatment modality in the field of dermatology. The efficacy of topical treatments depends on adequate drug deposition in the skin, and various strategies have been established to optimize cutaneous delivery, including ablative fractional lasers (AFXL), iontophoresis, microneedling, pressure, radiofrequency, and sonophoresis [1].

AFXL is rapidly evolving as one of the foremost techniques for cutaneous drug delivery [2–4]. AFXL generates microscopic ablation zones (MAZs) in the skin, consisting of vertical channels of ablated tissue [5,6]. The MAZs temporarily disrupt the skin-barrier and provide a pathway for uptake of topically applied drugs. Pretreatment with AFXL has proven to increase uptake of numerous topical agents, and the treatment of cutaneous malignancies has been the focus of foregoing research [7–11]. In clinical trials, AFXL-assisted photodynamic therapy has translated into more effective treatments for actinic keratoses (AK) [12–14].

AFXL is a highly customizable treatment encompassing adjustment of density, width, and depth of the channels to regulate drug deposition in the skin [15]. Deeper channels are expected to induce a greater dermal uptake, but inconsistent data on the influence of laser channel depth have been presented, indicating that deeper MAZs not always, but occasionally result in greater

**Conflicts of Interest Disclosures:** All authors have completed and submitted the ICMJE Form for Disclosure of Potential Conflicts of Interest and none were reported.

\*Correspondence to: Andrés M. Erlendsson, MD, Wellman Center for Photomedicine, Massachusetts General Hospital, Harvard Medical School, 50 Blossom Street, Their 2, Boston, MA 02114. E-mail: andres.erlendsson@gmail.com

Accepted 30 April 2015

Published online 17 August 2015 in Wiley Online Library (wileyonlinelibrary.com).

DOI 10.1002/lsm.22374

uptake [9,11,16,17]. To fully take advantage of channel depth, topically applied drugs must fill the space within the MAZs. However, interstitial fluid has been proposed to crowd the MAZs shortly after AFXL exposure, which may compromise spontaneous filling of the MAZs (Fig. 1). In addition, clinical trials examining AFXL-assisted photodynamic therapy for deep nodular basal cell carcinomas (BCC) have failed to significantly improve clearance rates with AFXL, potentially due to insufficient drug uptake in deep dermis [18]. Thus, in order to secure filling of the channels, and improve delivery, various methods to actively fill the MAZs may be of value.

Transient pressure waves and prolonged pressure application have been used to facilitate cutaneous drug delivery, and are suggested to improve delivery by transient permeabilization of stratum corneum (SC) and through naturally occurring appendageal ducts in the skin [19–21]. In view of previous studies, pressure may also be an applicable method to actively fill AFXL generated MAZs. Furthermore, alternating pressure and vacuum may mobilize tissue fluid present in the channels, and actively fill the channel with desired compound [21]. Once filled, the MAZ space can serve as a reservoir from which the drug can diffuse into dermis and improve bioavailability within the entire skin.

In this study, we sought to examine several aspects of AFXL-assisted drug delivery, investigating pressure and vacuum's impact on (i) relative filling of individual MAZs; (ii) cutaneous deposition and delivery kinetics; (iii) biodistribution and diffusion patterns, estimated by mathematical simulation.

## METHODS

### Study Set-Up

This study investigated a standardized method to actively fill AFXL-generated MAZs by altering pressure, vacuum and pressure (PVP) as illustrated in Figure 2. The study consisted of three separate parts, enquiring (i) relative filling of individual MAZs; (ii) cutaneous deposition and delivery kinetics for polyethylene glycol 400 (PEG400); and (iii) estimated bio-distribution by mathematical diffusion simulation. In Franz diffusion chambers (FCs; PermeGear Inc., Hellertown, PA), the relative filling of individual MAZs was investigated by delivering a green biomarker-liquid (Thermo Scientific™, Shandon™, Tissue Marking Dyes, Green) [22]. The biomarker binds permanently and unselectively through ionic bonds, thus visualizing if and how deep the material enters into the MAZs. Intracutaneous and transcutaneous deposition of a test molecule, polyethylene glycol (MW = 400 Da; PEG400), was investigated over time and quantified by nuclear magnetic resonance. Intradermal biodistribution and diffusion pattern for PEG400 were visualized in a two-dimensional mathematical simulation.

### Skin Preparation and Franz Chamber Mounting

Porcine skin was collected from the flank of female Yorkshire pigs immediately after euthanasia. Excessive hairs were trimmed and subcutaneous fat removed. FC's with a receptor volume of 5 ml and a permeation area of 0.64 cm<sup>2</sup> were filled with 0.9% saline and mounted with

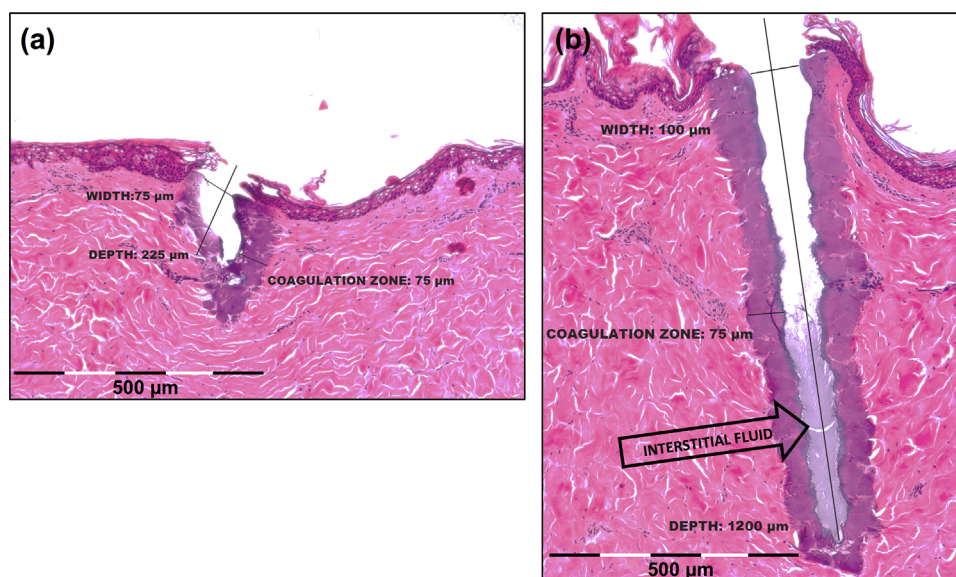


Fig. 1. Histology. Hematoxylin and eosin stained slides ( $\times 10$ ) depict superficial and deep laser channels generated by fractional CO<sub>2</sub> laser. (a) A pulse energy of 17.9 mJ/channel generated superficial channels penetrating 225  $\mu\text{m}$  deep with a diameter of 75  $\mu\text{m}$ , and 75  $\mu\text{m}$  coagulation zone. (b) The higher pulse energy, 130.5 mJ/channel generated deep channels penetrating 1,200  $\mu\text{m}$  into the skin with a diameter of 100  $\mu\text{m}$ , and a coagulation zone of 75  $\mu\text{m}$ . The arrow indicates interstitial fluid crowding spatial space within channel, potentially preventing compounds from filling into deep parts of the channel. The sample was fixated 30 minutes after laser exposure, suggesting that the influx of interstitial fluid starts shortly after laser exposure.

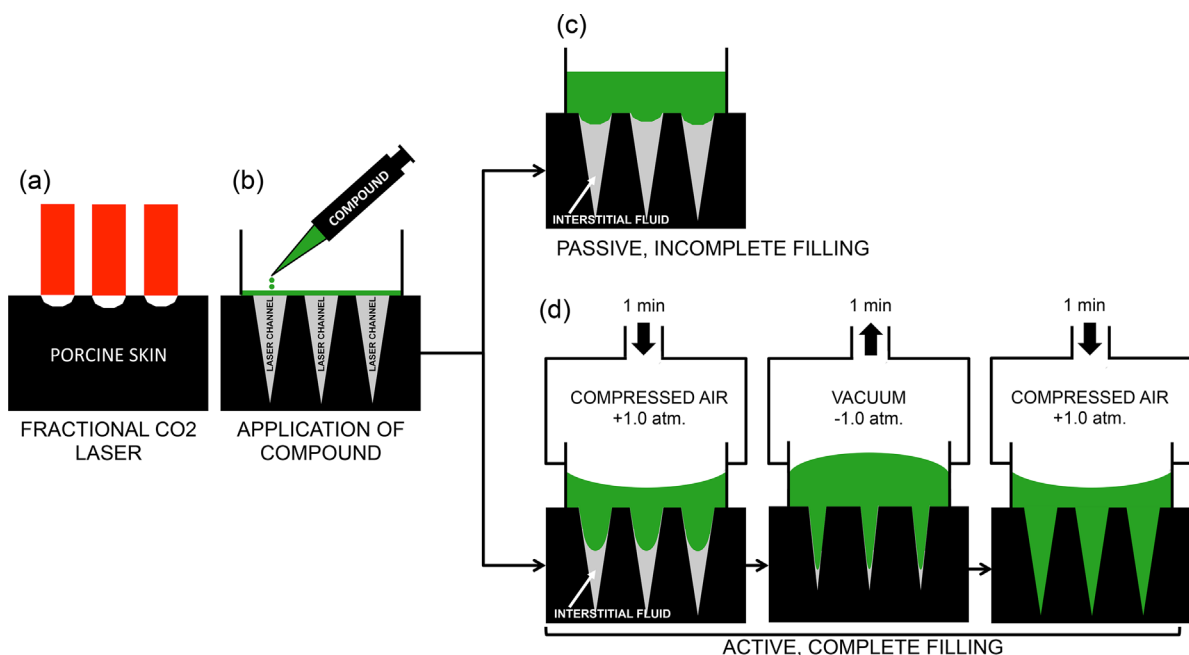


Fig. 2. Method: passive and active filling of laser channels. In porcine skin, a fractional CO<sub>2</sub> laser generates microscopic laser channels (a). After the laser treatment, skin samples were mounted in Franz diffusion chambers, and investigated compound applied in the donor chamber (b). Passive filling referred to spontaneous filling of the laser channels without any intervention (c). Active filling was conducted by applying a 3-minutes cycle of pressure (1 minute, +1.0 atm), vacuum (1 minute, -1.0 atm), and pressure (1 minute, +1.0 atm) (d).

porcine skin samples. Water at 37°C surrounded the FC-chambers and kept the skin temperature constant at 32°C, while magnetic stir bars stirred the receptor fluid.

### Laser and PVP Applications

AFXL was performed with a prototype CO<sub>2</sub> laser ( $\lambda = 10,600$  Solta, Palo Alto, CA) with a scanning device (48 series laser, SH Series Marketing Head, Model SH 3X-U/479, Synradinc., Mukilteo, WA) and a spot size of 200  $\mu\text{m}$ . A fixed density of 100 MAZs/cm<sup>2</sup> was used at two different pulse energies to generate superficial (17.9 mJ/MAZ, 0.5 ms, 35.8 W), and deep (130.5 mJ/MAZ, 5.0 ms, 26.1 W) MAZs. The superficial MAZs penetrated 225  $\mu\text{m}$  deep with an ablation diameter of 75  $\mu\text{m}$  and a surrounding 75  $\mu\text{m}$  coagulation zone. The higher pulse energy, 130.5 mJ/MAZ, generated deeper MAZs penetrating 1200  $\mu\text{m}$  deep with an ablation diameter of 100  $\mu\text{m}$  and a coagulation zone of 75  $\mu\text{m}$ .

Application of biomarker or PEG400 took place within 30 minutes of the AFXL treatment. In interventions assigned to PVP-application, a tube was attached to the donor chamber of the FC connecting it to a custom-made pressure-vacuum device (Fig. 2). The device delivered compressed air, creating a positive pressure of 1 atm, or vacuum, generating a negative pressure of 1 atm. After compound application (biomarker or PEG400), a three-minute cycle of 1 minute pressure, 1 minute vacuum, and 1 minute pressure was applied to the chamber.

### i - Filling of individual laser channels

A green biomarker liquid was delivered in skin samples with deep intradermal MAZs (1,200  $\mu\text{m}$ ) and interventions represented passive (AFXL,  $n = 6$ ), and active filling (AFXL + PVP,  $n = 6$ ; Table 1). After three minutes of active or passive filling, skin samples were embedded in OCT medium and stored at -80°C. Horizontal sections were photographed at depths of 100 and 1,000  $\mu\text{m}$ . In each sample, 49 channels were evaluated and filling was presented as the ratio of individually filled channels compared to total MAZs in the sample. In total, 588 MAZs were evaluated at both 100 and 1000  $\mu\text{m}$  skin depth.

### ii - Cutaneous deposition and delivery kinetics

Inracutaneous and transdermal uptake of PEG400 was investigated in intact skin and in AFXL-exposed skin with superficial and deep MAZs delivered with both passive and active filling (Table 2). Stock solutions of PEG400 10 mg/ml were prepared and 0.5 ml solution was applied directly on the skin in the donor chamber at  $t = 0$ . PVP was applied to assigned FCs, and diffusion ran for 10 minutes, 1 hour, and 4 hours. Parafilm (Bemis, Oshkosh, WI) covered the donor chambers to avoid desiccation of the skin. At the end of experiment, receiver solvent was collected for analyses of PEG400 uptake. The skin was washed with distilled water and padded dry with gauze prior to PEG extraction. To extract the PEG400, the skin was cut in four equal segments and placed in 3 ml 0.9% saline for 24 hours at 4°C.

**TABLE 1. Channel Filling With Liquid Biomarker**

|   | Passive filling (AFXL) |                                      |                          | Active filling (AFXL + PVP) |                                      |                          | <i>P</i> -value |
|---|------------------------|--------------------------------------|--------------------------|-----------------------------|--------------------------------------|--------------------------|-----------------|
|   | MAZs per sample        | Filled channels/total channels (IQR) | Filled channels, % (IQR) | MAZs per sample             | Filled channels/total channels (IQR) | Filled channels, % (IQR) |                 |
| Deep MAZs 1,200 $\mu\text{m}$<br>( <i>n</i> = 12 FCs, 588 MAZs) |                        |                                      |                          |                             |                                      |                          |                 |
| 100 $\mu\text{m}$   | 49                     | 47/49<br>(45–48)                     | 96%<br>(92–98%)          | 49                          | 49/49<br>(49–49)                     | 100%<br>(100–100%)       | 0.026           |
| 1,000 $\mu\text{m}$   | 49                     | 21/49<br>(18–22)                     | 44%<br>(37–46%)          | 49                          | 46/49<br>(46–47)                     | 94%<br>(94–96%)          | 0.002           |

Table presents median values with corresponding inter quartile range (IQR); AFXL, ablative fractional laser; PVP, pressure, vacuum, pressure; MAZs, microscopic ablation zones; *P*-values compare passive to active filling.

Aliquots from receptor and skin extraction solvents were placed in culture dishes and dried for 72 hours and then re-dissolved in deuterium oxide, with acetic acid as reference standard for NMR analyses. Spectra were recorded on a Bruker Biospin 300 MHz spectrometer (Bruker Ultrashield<sup>TM</sup> 300, Bruker Biospin AG, Fällanden, CH), and data were processed using Bruker TOPSPIN software version 2.1. For quantitative analysis of the PEG concentration, the area integral of the PEG's methylene proton signal at 3.6 ppm was compared to the reference signal area. The total uptake of PEG400 in skin and receiver was calculated by comparison to standards of 0.1, 1.0, and 10.0 mg/ml. Intracutaneous uptake was

presented as concentration in the tissue ( $\mu\text{g}/\text{ml}$ ) and transcutaneous uptake as absolute drug amount per skin surface area ( $\mu\text{g}/\text{cm}^2$ ). Tissue volume was estimated by micrometer measurement of skin thickness times the skin surface area ( $0.64 \text{ cm}^2$ ).

### iii - Mathematical simulation of PEG400 diffusion pattern

Two-dimensional diffusion of PEG400 in dermis was simulated in Matlab (Matlab 8.4.0, The Math Works, Inc., Natick, MA) for a grid of  $5 \times 5$  MAZs at a density of 100 MAZs/ $\text{cm}^2$  based on filling percentages at 1,000  $\mu\text{m}$

**TABLE 2. Intracutaneous and Transcutaneous Deposition of PEG400**

|   | Passive filling (AFXL) |                  |                     | Active filling (AFXL + PVP) |          |                  |          |                     |          |
|---|------------------------|------------------|---------------------|-----------------------------|----------|------------------|----------|---------------------|----------|
|   | 10 minutes (IQR)       | 1 hour (IQR)     | 4 hours (IQR)       | 10 minutes (IQR)            | <i>P</i> | 1 hour (IQR)     | <i>P</i> | 4 hours (IQR)       | <i>P</i> |
| Intact skin ( <i>n</i> )                        | 5                      | 6                | 6                   | .                           | .        | .                | .        | .                   | .        |
| Skin ( $\mu\text{g}/\text{ml}$ )                | 0<br>(0–0)             | 0<br>(0–0)       | 0<br>(0–0)          | .                           | .        | .                | .        | .                   | .        |
| Receiver ( $\mu\text{g}/\text{cm}^2$ )          | 0<br>(0–0)             | 0<br>(0–0)       | 0<br>(0–0)          | .                           | .        | .                | .        | .                   | .        |
| Superficial MAZs 225 $\mu\text{m}$ ( <i>n</i> ) | 5                      | 5                | 5                   | 6                           |          | 6                |          | 6                   |          |
| Skin ( $\mu\text{g}/\text{ml}$ )                | 0<br>(0–0)             | 118<br>(91–144)  | 544<br>(491–890)    | 0<br>(0–0)                  | 0.931    | 219<br>(178–262) | 0.009    | 808.6<br>(684–968)  | 0.429    |
| Receiver ( $\mu\text{g}/\text{cm}^2$ )          | 0<br>(0–0)             | 0<br>(0–0)       | 20.6<br>(0–34)      | 0<br>(0–0)                  | 1.000    | 0<br>(0–0)       | 1.000    | 36.6<br>(31–51)     | 0.329    |
| Deep MAZs 1,200 $\mu\text{m}$ ( <i>n</i> )      | 5                      | 5                | 5                   | 6                           |          | 6                |          | 6                   |          |
| Skin ( $\mu\text{g}/\text{ml}$ )                | 54<br>(0.0–77)         | 436<br>(413–439) | 1107<br>(1078–1372) | 303<br>(223–433)            | 0.004    | 601<br>(562–609) | 0.004    | 1114<br>(1096–1330) | 0.931    |
| Receiver ( $\mu\text{g}/\text{cm}^2$ )          | 0<br>(0–0)             | 0<br>(0–0)       | 32<br>(31–42)       | 0<br>(0–0)                  | 1.000    | 0<br>(0–7)       | 0.429    | 84<br>(70–118)      | 0.082    |

Table presents median values with corresponding inter quartile range (IQR). PEG400, polyethylene glycole; MW = 400 Da; MAZs, microscopic ablation zones. *P*-values compare passive to active filling.

depth from part I. The simulation was evaluated on a mesh created with the Matlab partial differential equation (PDE) tool over a finite domain of  $20 \times 20 \text{ mm}^2$  with a fine-grained mesh in the area covering the  $5 \times 5$  MAZs. Each MAZ had a diameter of  $100 \mu\text{m}$  and the start concentration of PEG400 in the MAZs was set to  $10 \text{ mg/ml}$ . PEG400 concentration at the domain boundaries was set to zero. The two-dimensional PDE describing changes in concentration ( $c$ ) at position vector ( $x$ ) over time ( $t$ ):  $\frac{\partial}{\partial t}c(x, t) = DK\nabla^2(x, t)$  was solved with a diffusion coefficient ( $D$ ) of  $6.0 \times 10^{-7} \text{ cm}^2/\text{s}$  and partition coefficient ( $K$ ) of 1.0. The diffusion coefficient was obtained from static diffusion of PEG400 through dermal tissue (data not shown). Simulation ran for 4 hours using finite element methods and plotted with Matlab triangular surface plot at 10 minutes, 1 hour, and 4 hours.

### Statistics

Nonparametric statistics compared filling percentages, depositions in skin, and receiver using Mann–Whitney  $U$  tests for two-group comparisons. Data were presented as medians with interquartile ranges (IQR).  $P$ -values were two-sided and considered statistically significant when less than 0.05. Statistical analyses were performed in SPSS version 20 (IBM Corporation, Armonk, NY).

## RESULTS

### Filling of MAZs With Active and Passive Filling

Filling percentages with and without PVP are presented in Table 1 and Figure 3. Passive filling of the laser channels was considerable at a superficial level, but incomplete in deeper parts of MAZs; at  $100 \mu\text{m}$  skin depth, the biomarker filled 96% of the channels, while only 44% were filled at  $1,000 \mu\text{m}$ . Active filling increased the number of filled channels and secured 100% filling at  $100 \mu\text{m}$  (AFXL vs. AFXL + PVP,  $P = 0.026$ ), and increased filling percentages from 44 to 96% at  $1,000 \mu\text{m}$  (AFXL vs. AFXL + PVP,  $P = 0.002$ ).

### Intracutaneous and Transcutaneous Delivery of PEG400

Intracutaneous deposition of PEG400 is presented in Table 2 and Figure 4. In intact skin, intracutaneous deposition of PEG400 was undetectable at all time points ( $0 \mu\text{g/ml}$ ; 10 minutes, 1 hour, and 4 hours).

Passive filling of superficial MAZs ( $225 \mu\text{m}$ ) generated a deposition of  $0 \mu\text{g/ml}$ ,  $118 \mu\text{g/ml}$ , and  $544 \mu\text{g/ml}$  at 10 minutes, 1 hour, and 4 hours, respectively. Applying PVP had no impact on delivery at 10 minutes ( $0 \mu\text{g/ml}$ ; AFXL vs. AFXL + PVP,  $P = 0.931$ ), but improved uptake at 1 hour and 4 hours, increasing concentrations to  $219 \mu\text{g/ml}$  ( $P < 0.009$ ) and  $809 \mu\text{g/ml}$  ( $P < 0.329$ ), respectively.

When deeper MAZs were applied ( $1,200 \mu\text{m}$ ), passive filling generated an uptake of  $54 \mu\text{g/ml}$  at 10 minutes,  $436 \mu\text{g/ml}$  at 1 hour, and  $1,106 \mu\text{g/ml}$  at 4 hours. Active filling greatly increased uptake, resulting in rapid build-up of high PEG400 concentrations in the skin. At 10 minutes, uptake was  $303 \mu\text{g/ml}$ , which was six times higher than with passive filling alone (AFXL vs. AFXL + PVP,

$P < 0.01$ ). The benefit of PVP was greatest at early time points, and decreased over time;  $600$  vs.  $435 \mu\text{g/ml}$  at 1 hour ( $P < 0.01$ ) and  $1,106$  versus  $1,113 \mu\text{g/ml}$  at 4 hours ( $P = 0.205$ ; Fig. 4).

Transdermal delivery was not detected at 10 minutes or 1 hour. At 4 hours, passive filling generated a transdermal uptake of  $21 \mu\text{g/cm}^2$  with superficial MAZs, and  $32 \mu\text{g/cm}^2$  with deep ( $P = 0.421$ ). Active filling with PVP increased transdermal deposition in both superficial and deep MAZs resulting in an uptake of  $37 \mu\text{g/cm}^2$  ( $P = 0.329$ ), and  $84 \mu\text{g/cm}^2$  ( $P < 0.082$ ), respectively. The increase was not statistically significant.

### Estimated Biodistribution of PEG400 in the Dermis

As depicted in Figure 5, the mathematical simulation of diffusion at  $1,000 \mu\text{m}$  depth revealed notable differences in both diffusion pattern and biodistribution of PEG400 when passive and active filling were compared. Passive filling left a majority of the MAZs empty (56%), resulting in an inhomogeneous uptake of PEG400 with low concentrations in the dermal tissue surrounding empty channels. The mottled uptake of PEG400 persisted throughout the entire simulation (0–4 hours), and left certain areas nearly unexposed to the compound (0–4 hours). Active filling with PVP secured a higher number of filled channels, and generated a greater and more uniform distribution within the entire dermal tissue (0–4 hours; Fig. 5).

## DISCUSSION

Active filling of MAZs may be a novel way to improve drug uptake in profound layers of the skin, potentially translating into more effective treatments of dermally invasive tumors.

In this study, we investigated a method to actively fill AFXL-generated channels, considering various aspects of the drug delivery process, including relative filling of individual MAZs, cutaneous and transdermal deposition of PEG400, as well as simulated bio-distribution in deep skin. Active filling with PVP secured channel filling in both superficial (100%) and deep (94%) portions of the MAZs, which led to a greater and more rapid deposition of PEG400 compared to passive filling. A mottled and inhomogeneous biodistribution was found with passive filling, which improved significantly with PVP and generated a uniform distribution within the deep dermal tissue.

SC is the main barrier preventing effective delivery of drugs through the skin [23]. SC consists of densely packed corneocytes embedded in a hydrophobic, nonpolar lipid matrix. Intact SC is nearly impermeable for most hydrophilic and charged molecules, as well as lipophilic molecules with molecular weight over 500 Da. Drugs designed for dermal and transdermal applications are therefore mostly small, moderately lipophilic, and partition readily into and out of SC.

The kinetics of topical drug delivery generally follows Fick's law of diffusion, which describes passive diffusion through a uniform planar medium. Fick's first law describes flux ( $J$ ) as  $J = (K \times D \times \Delta C)/L$ , where  $K$  is the partition coefficient,  $D$  is the diffusion coefficient,  $\Delta C$  is the

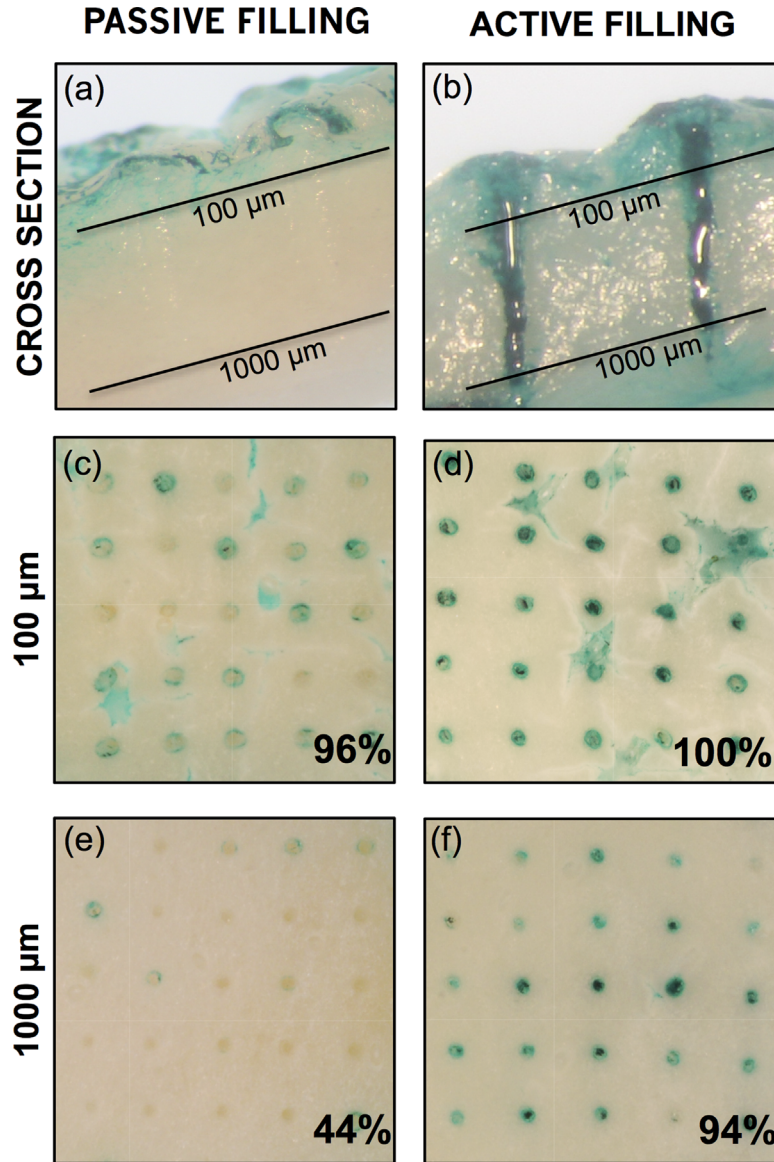


Fig. 3. Results: filling of MAZs with active and passive filling. The figure illustrates filling of the laser channels when delivering a green liquid biomarker with passive (a) and active filling (b). Passive filling of laser channels was considerable at a superficial level but incomplete in deeper parts of channels; at 100  $\mu\text{m}$ , the biomarker filled 96% of the channels (c), while only 44% were filled at 1,000  $\mu\text{m}$  (e). Active filling increased the number of filled channels and secured 100% filling at 100  $\mu\text{m}$  (d), and increased filling percentages from 44 to 96% at 1,000  $\mu\text{m}$  (f) (AFXL vs. AFXL + PVP,  $P < 0.01$ ).

concentration difference across the medium, and  $L$  is diffusion distance (length) [24]. While the concentration gradient over distance  $L$  drives the diffusion, the partition coefficient ( $K$ ) represents the equilibrium solubility of the drug at the skin surface relative to its solubility in the vehicle and is indicative of the drug's ability to leave the vehicle and enter the skin. The diffusion coefficient is a measure of a drug's diffusivity in a tissue matrix and determines the diffusion rate once the drug has entered into the skin. AFXL removes parts of SC and provides access through the channels to deeper skin layers where

the extracellular aqueous matrix resides, impacting flux in various ways.

Through Fick's law, it appears that AFXL will improve cutaneous uptake of a hydrophilic compound in three ways: (i) in areas where SC is removed, the partition ( $K$ ) between vehicle and skin is increased which enables the drug to leave the vehicle more easily than when applied to intact skin; (ii) once the compound leaves the vehicle, the drug enters directly into epidermis or dermis where the diffusivity is higher than in SC, thus facilitating the distribution of the compound in the tissue; and (iii) by

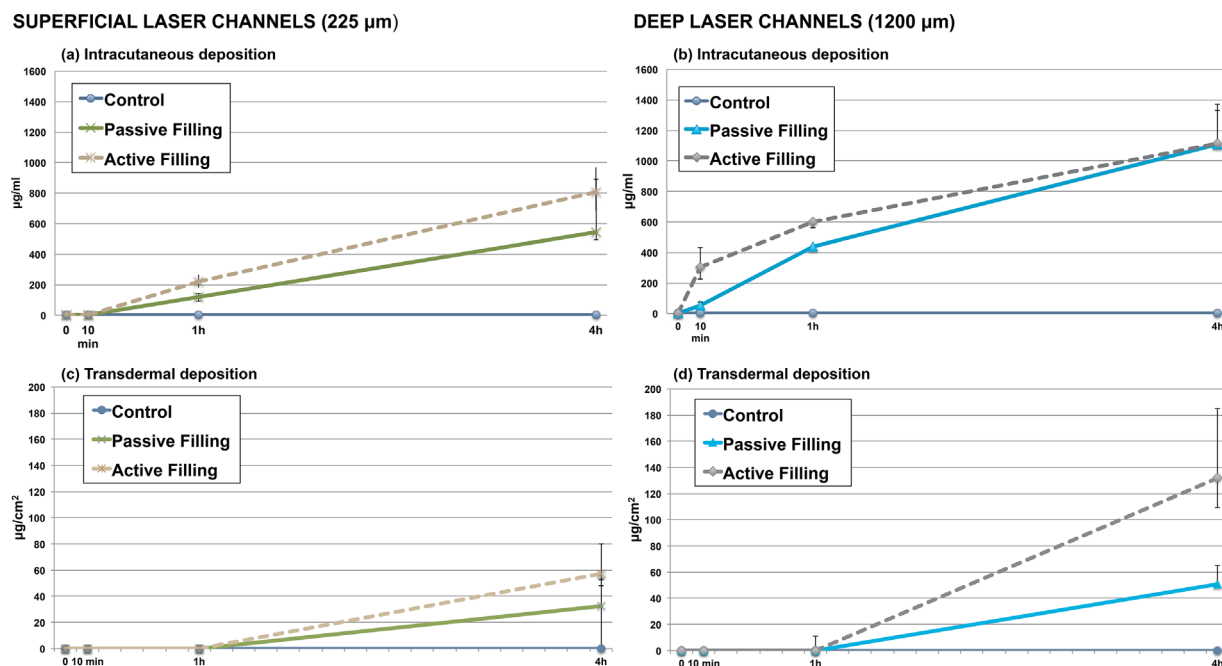


Fig. 4. Intracutaneous and transcutaneous deposition of PEG 400. The figures show intracutaneous (a,b) and transcutaneous (c,d) uptake of polyethylene glycol 400 Da (PEG400) in skin with superficial (225  $\mu\text{m}$ ) and deep (1,200  $\mu\text{m}$ ) laser channels delivered with active (AFXL + PVP) and passive (AFXL) filling. Applied to superficial channels, active filling with pressure vacuum pressure (PVP) had no impact on uptake at 10 minutes (0  $\mu\text{g}/\text{ml}$  AFXL vs. 0  $\mu\text{g}/\text{ml}$  AFXL + PVP,  $P = 0.931$ ), but generated a somewhat greater uptake at 1 hour (117  $\mu\text{g}/\text{ml}$  AFXL vs. 219  $\mu\text{g}/\text{ml}$  AFXL + PVP,  $P < 0.009$ ), and 4 hours (544  $\mu\text{g}/\text{ml}$  AFXL vs. 809  $\mu\text{g}/\text{ml}$  AFXL + PVP,  $P < 0.329$ ) (a). Applied to deep channels (1,200  $\mu\text{m}$ ), active filling generated a rapid build-up of PEG400 in the skin. After 10 minutes, PEG400-concentration reached 303  $\mu\text{g}/\text{ml}$ , which was six times higher than with AFXL alone (54  $\mu\text{g}/\text{ml}$ ; AFXL vs. AFXL + PVP,  $P < 0.01$ ) (b). Active filling with PVP increase transdermal deposition in both superficial (c) and deep (d) MAZs resulting in an uptake of 37  $\mu\text{g}/\text{cm}^2$  ( $P = 0.329$ ), and 84  $\mu\text{g}/\text{cm}^2$  ( $P = 0.082$ ), respectively. Data represents median values with corresponding interquartile range.

generating deep laser channels the distance the drug needs to diffuse is reduced, thus enabling delivery to deeper skin layers otherwise too distance from the skin surface to be affected by passive diffusion [22,24].

In this study, we investigated delivery of PEG400, a small, uncharged; and highly hydrophilic molecule (log  $P = -4.8$ ) [25]. As expected, PEG400 did not penetrate into or through intact skin at any time point. AFXL with passive filling (225  $\mu\text{m}$ ) provided direct access to viable skin, increasing the partition as well as the diffusivity for PEG400—both of which contributed to the great increase in intracutaneous deposition (0 vs. 543.6  $\mu\text{g}/\text{ml}$  at 4 hours). Increasing channel depth from 225 to 1200  $\mu\text{m}$  resulted in a greater cutaneous uptake at all time points (544 vs. 1106  $\mu\text{g}/\text{ml}$  at 4 hours).

Although deeper channels in theory are expected to generate a greater and possible deeper uptake, previous FC-studies have failed to agree on a relation between channel depth and drug deposition. *In vitro*, interstitial fluid and air has been found to occupy the MAZs after AFXL treatment. In addition, a recent *in vivo* study reported fibrin plug formation in the channels shortly after laser treatment [26]. Although the clinical implications of

these phenomena remain to be clarified, air, interstitial fluid, or fibrin plugs may prevent drugs and vehicles from filling into deep parts of the channels and thus prevent channel depth utilization.

In this study, delivery of PEG400 was found to increase with channel depth. The greater uptake observed with deeper MAZs may relate to the hydrophilicity of PEG400, which implies a low partition coefficient for entering into SC. The interstitial fluid present in the MAZs is likely to provide a more favorable environment for hydrophilic than hydrophobic drugs. Should the vehicle create an interface with the interstitial fluid, a hydrophilic molecule would readily partition from the vehicle into the interstitial fluid present in the MAZ, thereby utilizing MAZ depth. Such utilization may, however, only apply to hydrophilic compounds, as strongly lipophilic molecules will remain in the vehicle on the skin surface.

In support of this notion, previous FC-studies have observed a depth dependent uptake for hydrophilic compounds e.g., methotrexate, (log  $P = -1.85$ ) and slightly lipophilic compounds e.g., prednisone (log  $P = 1.46$ ) and diclofenac (log  $P = 1.90$ ) but not for hydrophobic drugs, such as lidocaine (log  $P = 2.44$ ),

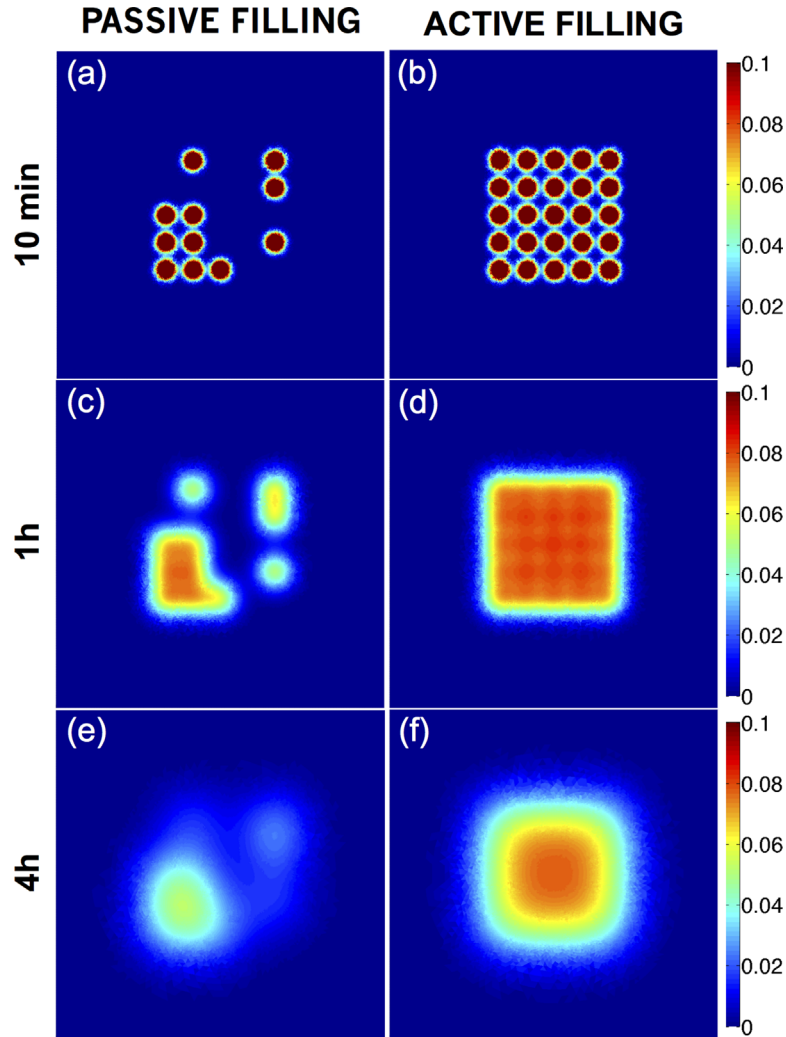


Fig. 5. Estimated biodistribution of PEG400 in the skin. The figure illustrates a simulated diffusion of polyethylene glycol 400 Da (PEG400) in dermis at a depth of 1000  $\mu\text{m}$  around a grid of 25 laser channels at 5% density depicted at 10 minutes (**a,b**), 1 hour (**c,d**), and 4 hours (**e,f**). Conventional ablative fractional laser-assisted drug delivery with passive filling resulted in an inhomogeneous distribution of PEG400, leaving some areas of the tissue almost unexposed to PEG400 (**a,c,e**). Active filling with PVP generated a predictable diffusion and resulted in a uniform distribution of PEG400 within the entire tissue (**b,d,f**).

ingenol mebutate ( $\log P=2.51$ ), and imiquimod ( $\log P=2.7$ ) [9,11,16,17,27–31].

For infinite dose models, like the FC model, the drug's solubility in the interstitial fluid may be a determining factor indicative of whether or not channel depth matters [24]. However, contrary to FC-studies, clinical applications include finite doses and when applied to patients, the vehicle may not remain on the skin surface long enough for the drug to partition into the fluid filled MAZs [24]. A more reliable way to achieve channel depth utilization is to fill the space within the MAZs, as demonstrated in this study.

Active filling with pressure and vacuum was used to create fluid flow into the laser channel, leading to rapid delivery of compounds deep into the dermis, securing channel filling in both superficial (100%) and deep (94%)

portions of the MAZs. Compared to passive filling, PVP did not notably increase filling percentages at a superficial level (AFXL 96% vs. AFXL + PVP 100%,  $P=0.026$ ) and had accordingly a nominal influence on cutaneous delivery through superficial MAZs.

Our study thus suggest that superficial MAZs intended to improve treatment for epidermal lesions may not benefit notably from PVP application; passive filling may suffice for those treatments. However, when applied to deep MAZs, PVP may be very useful; PVP increased channel filling from 44 to 94% ( $P=0.002$ ), which led to a six-fold increase in cutaneous uptake of PEG400 after only 10 minutes. Simulated bio-distribution within a deep dermal layer (1,000  $\mu\text{m}$ ) revealed benefits from the PVP application; the inhomogeneous distribution seen with passive filling was greatly improved with PVP and resulted in a

uniform uptake within the entire treatment area. Simply applying a drug after AFXL does not provide a predictable drug uptake when targeting deep dermal tumors. PVP appears to overcome this limitation.

Currently, even with AFXL-assisted drug delivery, topical treatments of BCCs are clinically challenging. A recent study comparing conventional photodynamic therapy (MAL-PDT) to AFXL-assisted PDT failed to significantly improve cure rates when treating high-risk nodular BCCs (63% AFXL PDT vs. 56% PDT) [18], potentially due to insufficient drug uptake in deep dermis.

PVP after AFXL secures filling of laser channels and induces a deeper, greater, and more rapid delivery than conventional AFXL. Active filling of AFXL-generated channels may be a novel way to improve drug uptake in profound layers of the skin, potentially translating into more effective treatments of dermally invasive tumors.

## ACKNOWLEDGMENTS

The authors wish to thank Erlendur Karlsson, MAM, MEE, PhD, Uppsala DSB Consulting, Uppsala, Sweden, for assistance with mathematical simulation of PEG400 diffusion, and Bradford D Ferrick, BS, Wellman Center for Photomedicine, Massachusetts General Hospital, Boston, Massachusetts 02114, for comments that greatly improved the manuscript.

## REFERENCES

- Brown MB, Martin GP, Jones SA, Akomeah FK. Dermal and transdermal drug delivery systems: Current and future prospects. *Drug Deliv* 2006;13(3):175–187.
- Bloom BS, Brauer JA, Geronemus RG. Ablative fractional resurfacing in topical drug delivery: An update and outlook. *Dermatol Surg* 2013;39(6):839–848.
- Sklar LR, Burnett CT, Waibel JS, Moy RL, Ozog DM. Laser assisted drug delivery: A review of an evolving technology. *Lasers Surg Med* 2014;262:249–62.
- Erlendsson AM, Anderson RR, Manstein D, Waibel JS. Developing technology: Ablative fractional lasers enhance topical drug delivery. *Dermatol Surg* 2014;40(Suppl 1):S142–S146.
- Manstein D, Herron GS, Sink RK, Tanner H, Anderson RR. Fractional photothermolysis: A new concept for cutaneous remodeling using microscopic patterns of thermal injury. *Lasers Surg Med* 2004;34(5):426–438.
- Hantash BM, Bedi VP, Chan KF, Zachary CB. Ex vivo histological characterization of a novel ablative fractional resurfacing device. *Lasers Surg Med*. 2007;39(2):87–95.
- Haedersdal M, Sakamoto FH, Farinelli WA, Doukas AG, Tam J, Anderson RR. Fractional CO<sub>2</sub> laser-assisted drug delivery. *Lasers Surg Med* 2010;42(2):113–22.
- Lee W-R, Shen S-C, Pai M-H, Yang H-H, Yuan C-Y, Fang J-Y. Fractional laser as a tool to enhance the skin permeation of 5-aminolevulinic acid with minimal skin disruption: A comparison with conventional erbium:YAG laser. *J Control Release* 2010;145(2):124–133.
- Lee W-R, Shen S-C, Al-Suwayeh SA, Yang H-H, Yuan C-Y, Fang J-Y. Laser-assisted topical drug delivery by using a low-fluence fractional laser: Imiquimod and macromolecules. *J Control Release* 2011;153(3):240–248.
- Bachhav YG, Heinrich A, Kalia YN. Using laser microporation to improve transdermal delivery of diclofenac: Increasing bioavailability and the range of therapeutic applications. *Eur J Pharm Biopharm* 2011;78(3):408–414.
- Haak CS, Farinelli WA, Tam J, Doukas AG, Anderson RR, Haedersdal M. Fractional laser-assisted delivery of methyl aminolevulinic acid: Impact of laser channel depth and incubation time. *Lasers Surg Med* 2012;44(10):787–795.
- Helsing P, Togsverd-Bo K, Veierød MB, Mørk G, Haedersdal M. Intensified fractional CO<sub>2</sub> laser-assisted photodynamic therapy vs. laser alone for organ transplant recipients with multiple actinic keratoses and wart-like lesions: A randomized half-side comparative trial on dorsal hands. *Br J Dermatol* 2013;169(5):1087–1092.
- Togsverd-Bo K, Haak CS, Thaysen-Petersen D, Wulf HC, Anderson RR, Haedersdal M. Intensified photodynamic therapy of actinic keratoses with fractional CO<sub>2</sub> laser: A randomized clinical trial. *Br J Dermatol* 2012;166(6):1262–1269.
- Togsverd-Bo K, Lei U, Erlendsson AM, Taudorf EH, Philipsen PA, Wulf HC, Skov L, Haedersdal M. Combination of ablative fractional laser and daylight-mediated photodynamic therapy for actinic keratosis in organ transplant recipients—a randomized controlled trial. *Br J Dermatol* 2015;172(2):467–474.
- Taudorf EH, Haak CS, Erlendsson AM, Philipsen PA, Anderson RR, Paasch U, Haedersdal M. Fractional ablative erbium YAG laser: Histological characterization of relationships between laser settings and micropore dimensions. *Lasers Surg Med*. 2014;46(4):281–289.
- Oni G, Brown S a, Kenkel JM. Can fractional lasers enhance transdermal absorption of topical lidocaine in an *in vivo* animal model? *Lasers Surg Med* 2012;44(2):168–174.
- Yu J, Bachhav Y, Summer S, Heinrich A, Bragagna T, Böhler C, Kalia YN. Using controlled laser-microporation to increase transdermal delivery of prednisone. *J Control Release* 2010;148:e71–e73.
- Haak C, Togsverd-Bo K, Thaysen-Petersen D, Wulf H, Paasch U, Anderson R, Haedersdal M. Fractional laser-mediated photodynamic therapy of high-risk basal cell carcinomas—a randomized clinical trial. *Br J Dermatol* 2014;172(1):215–222.
- Lee S, Mcauliffe DJ, Flotte TJ, Kollias N, Doukas AG. Photomechanical transcutaneous delivery of macromolecules. *J Invest Dermatol* 1998;11(6):925–930.
- Doukas AG, Kollias N. Transdermal drug delivery with a pressure wave. *Adv Drug Deliv Rev* 2004;56(5):559–579.
- Treffel P, Panisset F, Humbert P, Remoussenard O, Bechtel Y, Agache P. Effect of pressure on *in vitro* percutaneous absorption of caffeine. *Acta Derm Venereol* 1993;73(3):200–202.
- Franz TJ. Percutaneous absorption on the relevance of *in vitro* data. *J Invest Dermatol* 1975;64:190–195.
- Elias PM, Menon GK. Structural and lipid biochemical correlates of the epidermal permeability barrier. *Adv Lipid Res* 1991;24:1–26.
- Franz TJ. Kinetics of cutaneous drug penetration. *Int J Dermatol* 1983;22(9):499–505.
- Ma T, Hollander D, Krugliak P, Katz K. PEG 400, a hydrophilic molecular probe for measuring intestinal permeability. *Gastroenterology* 1990;98(1):39–46.
- Kositratna G, Manstein D. Rapid fibrin plug formation within ablative fractional CO<sub>2</sub> laser lesions. *LASER ASLMS Conference*. 2015. p. Abstract # 88.
- Saaidpour S. Prediction of drug lipophilicity using back propagation artificial neural network modeling. *Orient J Chem* 2014;30(2):793–802.
- Scheytt T, Mersmann P, Lindstadt R, Heberer T. 1-Octanol/water partition coefficients of 5 pharmaceuticals from human medical care: Carbamazepine, clofibrac acid, diclofenac, ibuprofen, and propyphenazone. *Water Air Soil Pollut* 2005; 165:3–11.
- Leo A, Hansch C, Elkins D, Law AH, Behavior BN. Partition coefficients and their uses. *Chem Rev* 1971;71(6):525–615.
- Taudorf E, Lerche C, Vissing A, Philipsen P, Hannibal J, D'Alvise J, Hansen S, Janfelt C, Paasch U, Anderson R, Haedersdal M. Topically applied methotrexate is rapidly delivered into skin by fractional laser ablation. *Expert Opin Drug Deliv* 2015;12(7):1059–1069.
- Erlendsson AM, Taudorf EH, Eriksson AH, Haak CS, Zibert JR, Paasch U, Anderson RR, Haedersdal M. Ablative fractional laser alters biodistribution of ingenol mebutate in the skin. *Arch Dermatol Res* 2015; [Epub ahead of print].